



Assessment of aquifer protective strength and groundwater quality within the University of Nigeria, Nsukka campus using geophysical and laboratory techniques

J. A. Yakubu¹ · N. A. Okwesili¹ · J. C. Ibuot¹ · D. N. Obiora¹

Received: 16 December 2021 / Accepted: 13 June 2022 / Published online: 12 July 2022

© The Author(s), under exclusive licence to Iranian Society of Environmentalists (IRSEN) and Science and Research Branch, Islamic Azad University 2022

Abstract

The study integrates geophysical and geochemical methods so as to evaluate the protective strength and the quality of groundwater within the Nsukka campus of the University of Nigeria. Thirteen vertical electrical sounding (VES) points help in delineating the subsurface strata resulting to five geoelectric layers. The values of aquifer resistivity and thickness were used in estimating the longitudinal conductance, transverse resistance, hydraulic conductivity and transmissivity. The longitudinal conductance ranged from 0.018 to 0.093 Ω^{-1} , transverse resistance ranged from 91,370.52 to 772,493.50 Ωm^2 , while hydraulic conductivity and transmissivity ranged from 0.1209 to 0.5405 m/day and 12.3988 to 58.0114 m^2/day , respectively. These parameters illustrate the hydrogeologic characteristics of the aquifer units. The analysis and interpretation of the water samples revealed that the concentration of the total dissolved solute (TDS), cations and anions were below the World Health Organisation standard (WHO), the only exception was Fe^{2+} that exceeded limit in some boreholes. The Magnesium Hazard (MH), Sodium Adsorption Ratio (SAR) and Sodium percentage (Na%) show the irrigation suitability of the groundwater of the area in order to boost agricultural yield.

Keywords Geochemical ions · Hydrogeologic · Suitability · Resistivity · WHO

Introduction

Water, a natural resource, plays a major role in the sustainability of man, animals, and plants, but its quality keeps degrading, and this has been a major concern in recent years. This according to UNESCO endangers human health, affects the economic growth of a country and equally leads to food insecurity. The degradation may be attributed to urbanization, industrialization, and an over-populated world, and the effect has attracted a lot of attention due to its overwhelming environmental significance (George, 2021; Ibuot et al., 2019; Verma et al., 2020; Yan et al., 2015) and also put more pressure on water resources (Chandra et al., 2015). Groundwater quality depends upon the chemical constituents and their concentrations, and also the crevices and pore spaces of the subsurface rocks and soils, which allow infiltration

of pollutants into the aquifer layer, thereby changing the electrical, chemical, and physical properties of groundwater repositories. The contaminant fluid is loaded with mobile ions rich in mineral nutrients that are required by plants for agricultural productivity. The contaminant-loaded groundwater is not good for consumption due to the degradation (Ibuot et al., 2017; Thomas et al., 2020).

Contaminants emanating from dumpsites, sewage sites, fertilizers, etc. affect groundwater quality and penetrate the subsurface aquifers through the pores and crevices of rocks and soils after decomposition, becoming point sources of groundwater pollution (Hossain et al., 2014; Ganiyu et al., 2015; Ibuot et al., 2017). The sources of these contaminants have become difficult to manage since many charged with that responsibility fail to understand the complex processes of waste in the soil. According to researchers (George et al., 2015; Ibuot et al., 2019; Thomas et al., 2020), the degree of groundwater contamination is less than that of surface water since the earth materials act as filters for percolating fluids. Since the percolating fluids still get to the aquifer layers over time, there is a need for hydrogeochemical analysis of groundwater in order to understand the type of chemical

✉ N. A. Okwesili
ngozi.okwesili@unn.edu.ng

¹ Department of Physics and Astronomy, University of Nigeria, Nsukka, Nigeria

species present in the aquifer systems as a result of the percolating fluids. The composition of the shallow subsurface affects water balance, e.g. permeation and retention. Geologically, the overburden layers that allow the percolation of surface contaminants in the aquifer repositories can be studied using the electrical resistivity method, which displays the conductivity or resistivity of the distributed arenaceous or argillaceous geological formations vertically and horizontally (George et al., 2015; Obiora & Ibuot, 2020; Oguama et al., 2019). The electrical resistivity method delineates geologic formation properties that are important to hydrogeology and correlates with the electrical conductivity signatures of the aquifer repositories. The large contrast in electrical conductivity contrast of most contaminants to that of groundwater helps in detecting contaminating plumes using the electrical resistivity method (Akpan et al., 2013; Obiora et al., 2015).

The present study is an attempt to delineate the subsurface geologic layering and the groundwater chemistry by integrating electrical resistivity measurements and laboratory analysis of water samples within the study area comparison. The objective of this study is to use the electrical resistivity technique to assess the protective capacity of the

hydrogeologic units and also the suitability of the groundwater for domestic and irrigation purposes through the analysis of hydrogeochemical facies. This research will aid in the delineation of the protective zone and will also serve as a guide for groundwater resource management.

Location and geology of the study area

The study area lies between longitudes $7^{\circ} 0' 0''$ E and $8^{\circ} 0' 0''$ E, and Latitude $6^{\circ} 0' 0''$ N and $7^{\circ} 0' 0''$ N (Fig. 1) and is found within the Ajali and Nsukka geological Formations (Fig. 2). A shaly impermeable unit of the Mamu Formation underlies the Ajali Formation, trapping the Ajali aquifers. The Ajali Sandstone, which is the upper Maastrichtian, is about 451 m thick (Omeje et al., 2021), and is composed of poorly consolidated sandstone characteristically cross-bedded with minor clay layers. The thickness of the aquifer unit varies from one location to another as it moves from shallow to deep (Omeje et al., 2021). The weathered top of the Ajali Sandstone provides the appropriate environment for water storage, which allows for high permeation rate and high permeability. The lithology of Nsukka consists of fine-medium

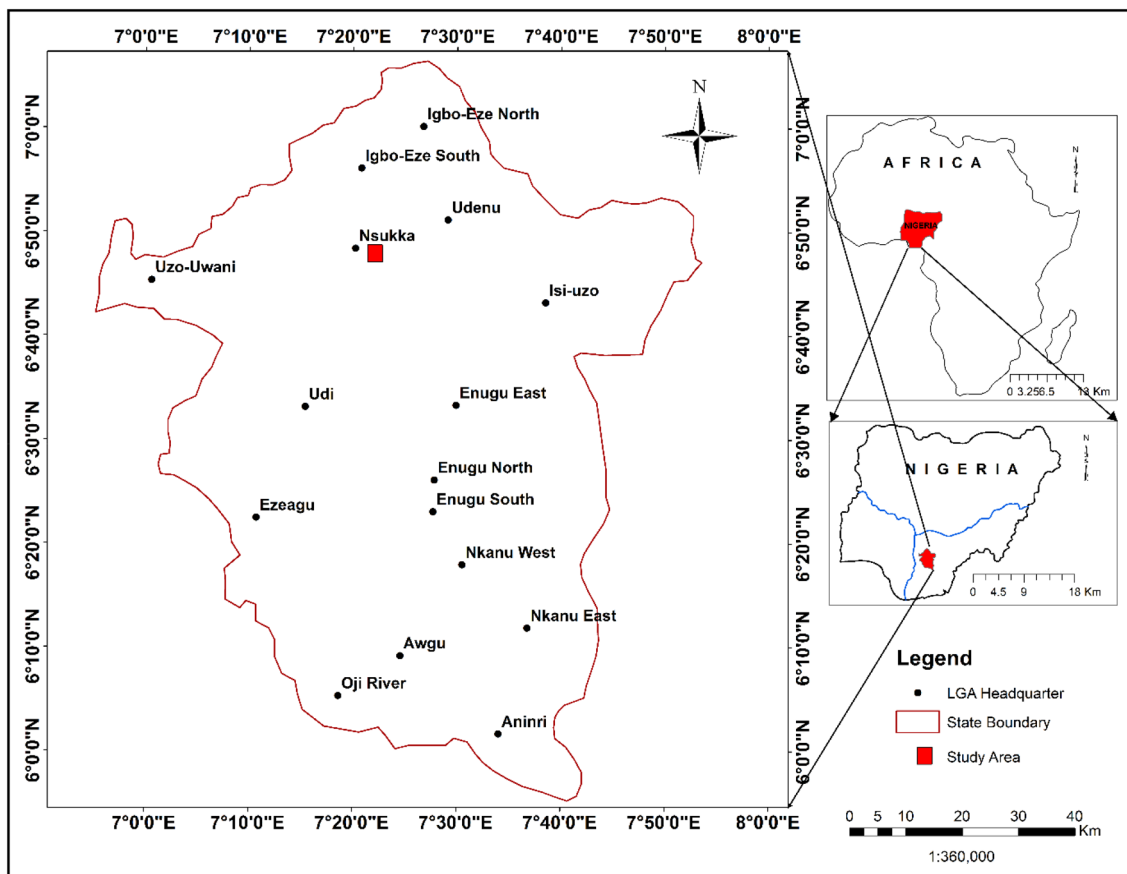


Fig. 1 Map showing the location of the study area

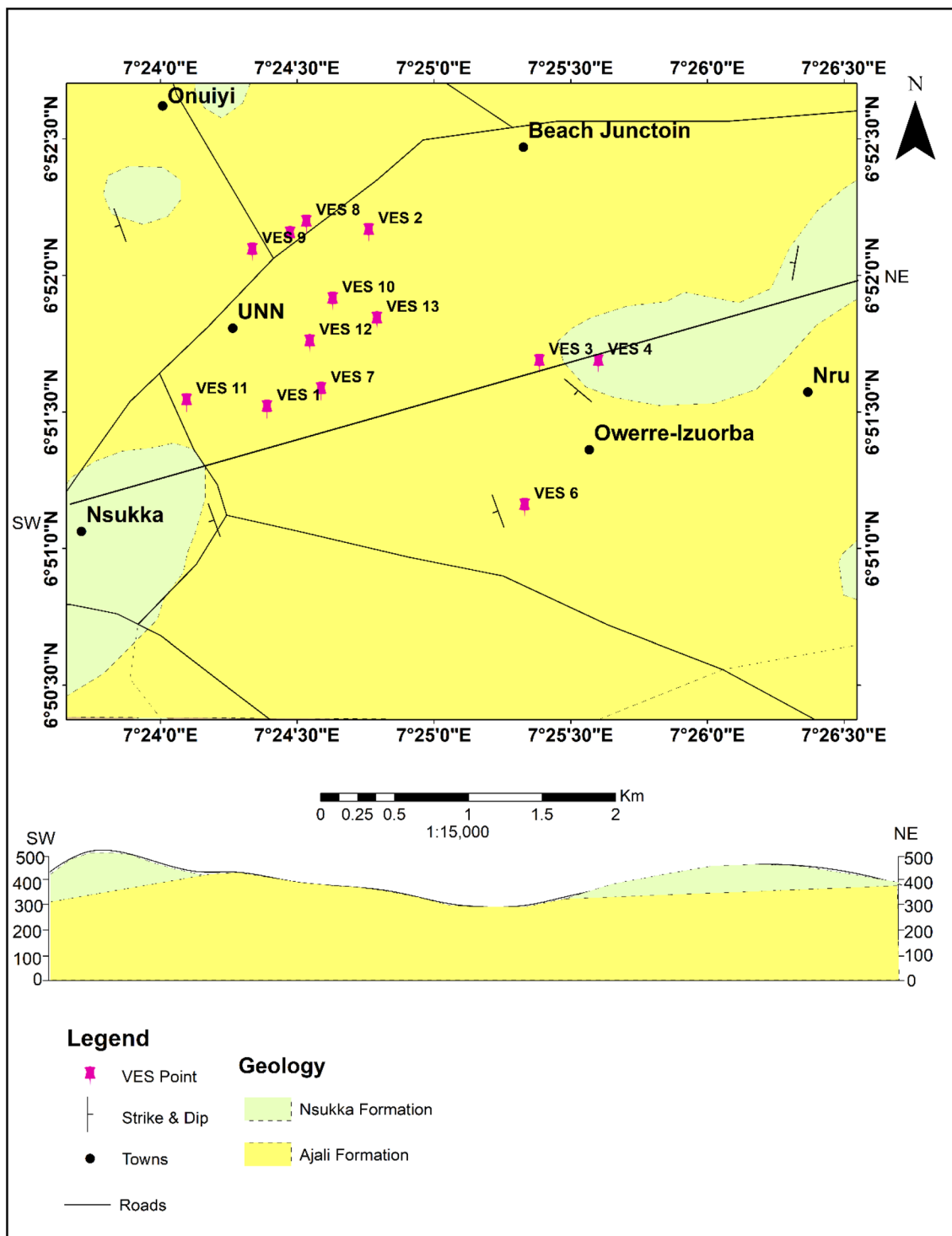


Fig. 2 Geologic map of the study area showing the VES points

grained sandstones, carbonaceous shale, clay, siltstone, and bands or seams of impure coal interbedded in shales and siltstones (Reyment, 1965; Simpson, 1954), which have developed lateritized in various locations and typically form resistant coverings on mesas and buttes. The Nsukka

Formation is physiographically dotted by many cone-shaped hills separated by low lands and broad valleys and are laterite-covered (Obaje, 2009). An important topographical feature found in the study area is the North–South trending cuesta over Ajali sandstone.

Materials and methods

The resistivity method makes use of Schlumberger electrode configuration and vertical electrical sounding (VES). The resistivity survey measures the potentials between pairs of electrodes as current is transmitted between another pair of electrodes. This method is suitable for studying the lithological characteristics of the subsurface strata and the variations of electrical properties (George et al., 2016; Ibutot & Obiora, 2021). This integrated study involves the use of surface resistivity and geochemical methods in assessing the groundwater quality within the study area. Thirteen (13) soundings were carried out, and the current electrode spread of 800 m was measured using an IGIS resistivity meter. Direct current is injected into the subsurface via a pair of current electrodes and the potential difference across the potential electrodes is measured. The apparent resistivity (ρ_a) was computed from Eq. 1.

$$\rho_a = \pi \cdot \left[\frac{\left(\frac{AB}{2}\right)^2 - \left(\frac{MN}{2}\right)^2}{MN} \right] \cdot R_a \tag{1}$$

where AB and MN are the current electrodes distance and the potential electrodes distance, while R_a is measured resistance. Equation 1 can be reduced to Eq. 2;

$$\rho_a = K \cdot R_a, \tag{2}$$

where K represent the geometric factor: $\pi \cdot \left[\frac{\left(\frac{AB}{2}\right)^2 - \left(\frac{MN}{2}\right)^2}{MN} \right]$.

The global positioning system (GPS) was used in measuring the longitudes and latitudes of each location. The bi-logarithm graph was used to plot the values of ρ_a against $\frac{AB}{2}$

and the curves obtained were smoothed in order to remove the noisy signatures which do not follow the usual curve trend. The smoothing was achieved by either taking the mean of two readings taken at the points of crossover or by simply discarding some points that were not consistent with the prevailing curve trend. The curves were quantitatively interpreted by conventional manual curves and auxiliary charts to give the true resistivity and thickness. This was improved upon by the use of the WinResist software package, and this gives the modelled geological curves for each VES point, and Figs. 3 and 4 are some of the curves generated. The WinResist software program gives information on the interpreted curve by defining the layer resistivity, layer thickness, and layer depth and the root-mean square (RMS), which defines the degree of goodness of fit between the theoretical curve and the curve of the field data. The primary geoelectric parameters (resistivity and thickness) were used in calculating the longitudinal conductance and transverse resistance, which are together referred to as the Dar-Zarrouk parameters. Also, other parameters (hydraulic conductivity and transmissivity) that describe the hydrogeologic properties of the subsurface were determined from the primary geoelectric parameters.

The longitudinal conductance (S) which determines the degree of susceptibility of the saturated layers was computed using Eq. 3;

$$S = \frac{h}{\rho} \tag{3}$$

While the transverse resistance (T) was computed from Eq. 4:

$$T = \rho h, \tag{4}$$

Fig. 3 Geological curves at VES 1

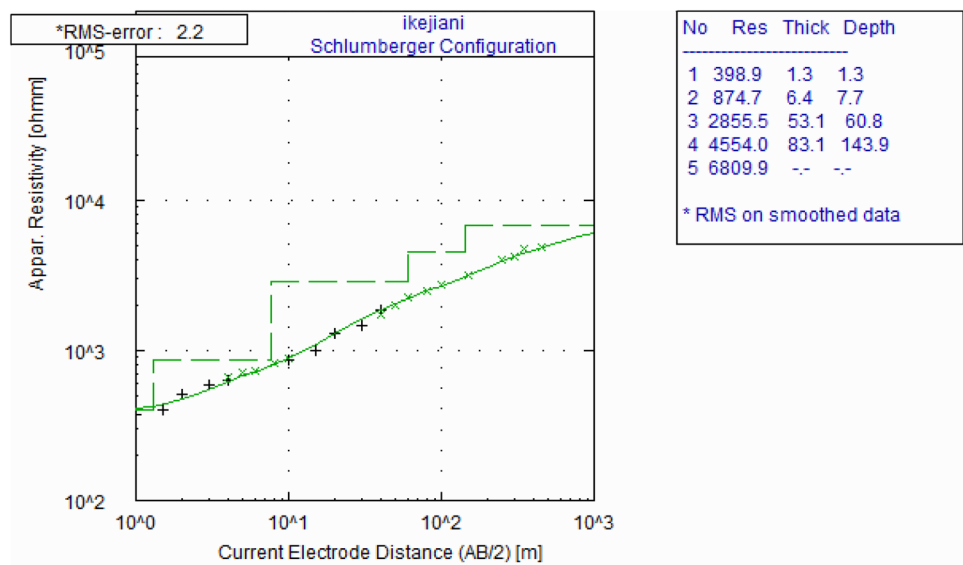
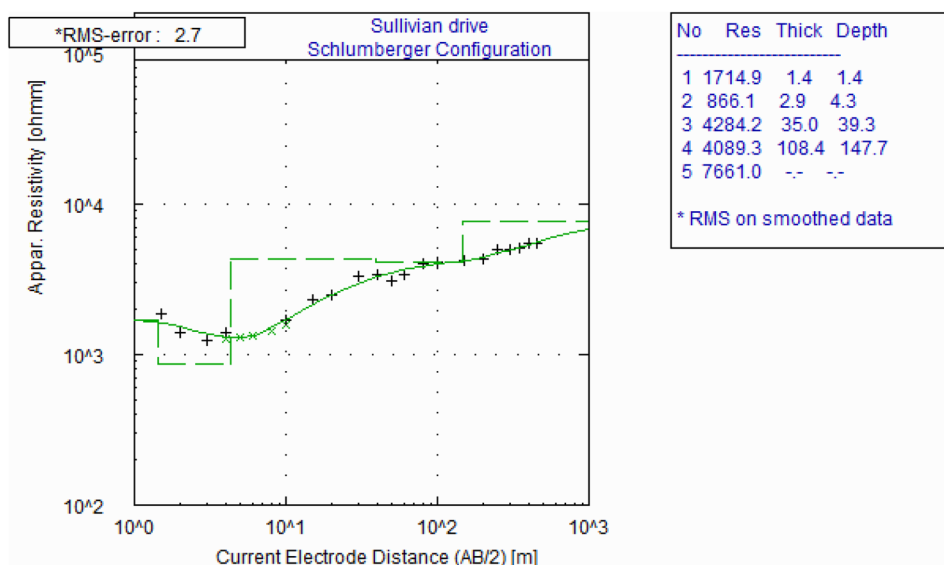


Fig. 4 Geological curves at VES 2



where ρ and h are resistivity and thickness of each layer, respectively. The earth’s medium has the ability to retard and sieve infiltrating fluids, which is a measure of its protective strength (Obiora et al., 2015). The computed longitudinal conductance aids in the classification of the aquifer repositories based on their protective strength according to Oladapo et al. (2004), and the area can be classified into poor, weak, moderate, good, very good, and excellent based on its longitudinal values.

Hydraulic conductivity (K) defines the ease at which fluids travel through the porous spaces of rocks. It was computed using Eq. 5 according to Ibuot et al. (2019), who worked in a similar geologic terrain.

$$K = 386.42\rho^{-.93} \tag{5}$$

where ρ , is the aquifer resistivity in Ωm . The hydraulic conductivity describes the ability of an aquifer to permit the flow of groundwater. This property (K), according to Aleke et al. (2018), impacts on well/borehole productivity and the velocity at which contaminants spread. The transmissivity of the aquifer units defines the degree of pore-water flow per day. It was computed from Eq. 6, and it relates both the hydraulic conductivity (K) and the thickness (h) of the hydrogeologic layer.

$$T_r = Kh. \tag{6}$$

The laboratory analysis involved five (5) different water samples obtained from different boreholes at different locations in the study area. The essence of the laboratory analysis was to determine the concentrations of some cations and anions using the Atomic Absorption

Spectrophotometer (UNICAM 969AAS) and the DR 2000 Spectrophotometer, respectively. Using phenolphthalein and methyl orange indicator, the concentrations of the carbonates and bicarbonates (CO_3^{2-} and HCO_3^-) were generated using standard procedure of titrimetric method. To prevent the metallic ions from sticking to the walls of the container and to homogenize the water samples, the water for anion determination was acidified with nitric acid (HNO_3). The total dissolved solute (TDS) was determine using the gravimetric method. The values of the concentrations of the various parameters analysed were compared with the World Health Organisation (WHO) standard (WHO 2004), so as to evaluate the health risks to human beings.

The suitability of groundwater for agriculture was determined using the concentrations of sodium, calcium, potassium and magnesium (Raghunath, 1987; Sisir & Anindita, 2012). The indicators; Magnesium Hazard (MH), Sodium Adsorption Ratio (SAR), and Sodium percentage (Na%) were computed using Eqs. 7, 8 and 9.

$$MH = \frac{Mg^{2+}}{Ca^{2+} + Mg^{2+}} \times 100, \tag{7}$$

$$SAR = \frac{Na^+}{\sqrt{\frac{Ca^{2+} + Mg^{2+}}{2}}}, \tag{8}$$

$$Na\% = \frac{Na^+ \times 100}{(Ca^{2+} + Mg^{2+} + Na^+ + K^+)}, \tag{9}$$

where Na^+ , Mg^{2+} , K^+ and Ca^{2+} are sodium, magnesium, potassium and calcium ions, respectively.

Results and discussion

VES results

The result of the electrical resistivity survey (VES) carried out within the study area is presented in Table 1. The result shows a wide range of resistivity of the subsurface materials, with five layers obtained across the study area within the maximum current electrode separation. The resistivity of the first layer, the top soil has a resistivity ranging from 196.6 to 4884.9 Ωm with its thickness and depth ranging from 0.7 to 5.4 m. This layer on the average may be lateritic in nature. The resistivity of the second and third geoelectric layers was found to range from 42.3 to 7208.6 Ωm and 61.1 to 16,724.1 Ωm , respectively. The fourth layer, which is underlain by the third layer, harbours the aquifer in the study area has resistivity which ranges from 1146.1 to 5713.3 Ωm , its thickness and depth range from 71.9 to 184.3 m and 120.3 to 198.5 m, respectively. The thickness of this layer is high compared to the overlain layers and may be said to comprise medium-coarse grained sand. The fifth geoelectric layer with resistivity range of 781.7 to 33,327.2 Ωm with its thickness and depth undefined. The observed wide variation in values of resistivity may be due to the effect of infiltration of geofluids into the subsurface strata and this may contribute to the low resistivity values of the topmost layers (George, 2021; Ibuot et al., 2019; Obiora et al., 2016).

The aquifer resistivity and thickness were used to compute the longitudinal conductance and transverse resistance, hydraulic conductivity, and transmissivity of the aquifer layers (Table 2). The resistivity and thickness vary from 1146.1 to 5713.3 Ωm and 71.9 to 184.3, respectively.

The major factor affecting the results of the resistivity test in this study is the nature of the subsurface geologic materials in the study area, since the resistivity of earth materials depends on factors such as density, shape, size, pore size, water content, clay, and porosity of the constituent geologic materials (Choudhury & Saha, 2004; Ekanem et al., 2021; Ibuot et al., 2021). The longitudinal conductance (S) describes the degree of susceptibility of the aquifer has values varying from 0.018 to 0.093 Ω^{-1} . This shows a poor-weak protective strength according to the ratings of Oladapo et al. (2004), which indicates that the aquifer unit is susceptible to contamination from surface contaminants percolating into the subsurface overtime. The transverse resistance (T) ranges from 91,370.52 to 772,493.5 Ωm^2 , the high values are attributed high thickness and this may influence aquifer yield. The hydraulic conductivity (K) ranges from 0.121 to 0.541 m/day indicating the ease with which fluids percolates into the subsurface. The product of thickness and hydraulic conductivity give the aquifer transmissivity which values ranges from 12.399 to 58.011 m^2/day , indicating low to moderate groundwater potential zone. These parameters were contoured in order to display their variations across the study area. Figures 5 and 6 are contour maps showing the variations of aquifer resistivity and thickness. High values of these parameters are observed in the northern part, and they decrease towards the south. The region with high resistivity may be as a result of low conductive earth materials, which is attributed to infiltration from surface contaminants.

The longitudinal conductance was contoured and the contour map (Fig. 7) shows the variations of this parameter. The northeastern and southwestern zones of the study area have low longitudinal conductance, indicating that these zones are more permeable and more susceptible to contamination from surface contaminants, which

Table 1 Electrical resistivity result for the thirteen VES locations

VES	Longitude (°E)	Latitude (°N)	Layer resistivity (Ωm)					Thickness (m)					Depth (m)				
			ρ_1	ρ_2	ρ_3	ρ_4	ρ_5	h_1	h_2	h_3	h_4	h_5	d_1	d_2	d_3	d_4	d_5
1	7.4065	6.8585	398.9	874.7	2855.5	4554.0	6809.9	1.3	6.4	53.1	83.1	–	1.3	7.7	60.8	143.9	–
2	7.4127	6.8693	422.3	2553.3	2455.6	5713.9	7118.9	1.5	9.0	35.7	104.6	–	1.5	10.5	46.2	150.8	–
3	7.4231	6.8613	1714.9	866.1	4284.2	4089.3	7661.0	1.4	2.9	35.0	108.4	–	1.4	4.3	39.3	147.7	–
4	7.4267	6.8613	3108.3	756.2	2714.2	3211.7	33,327.2	0.9	3.2	46.1	109.8	–	0.9	4.0	50.2	160.0	–
5	7.4079	6.8691	626.1	185.7	14,163.8	2799.0	2086.4	1.4	2.9	28.3	114.9	–	1.4	4.4	32.7	147.6	–
6	7.4222	6.8525	331.6	103.5	2212.0	2339.0	4332.0	2.8	4.6	7.1	137.3	–	2.8	7.4	14.5	151.8	–
7	7.4098	6.8596	196.6	760.9	320.2	1146.1	3617.1	0.7	7.1	14.2	98.2	–	0.7	7.8	22.1	120.3	–
8	7.4089	6.8698	547.4	870.6	1125.9	4261.6	1322.4	3.2	7.4	15.8	117.2	–	2.2	10.6	26.4	143.6	–
9	7.4056	6.8681	4884.9	7208.6	3993.5	1523.9	1094.3	5.0	8.3	25.8	86.9	–	5.0	13.3	39.1	126.0	–
10	7.4105	6.8651	408.3	1266.1	61.1	4191.5	2598.5	1.0	2.0	11.1	184.3	–	1.0	3.0	14.1	198.5	–
11	7.4016	6.8589	798.9	258.8	3847.1	2042.3	3901.3	1.8	9.2	12.8	138.7	–	1.8	11.0	23.5	162.2	–
12	7.4091	6.8625	393.4	42.3	16,724.1	1246.8	821.5	1.8	2.3	39.5	116.1	–	1.8	4.1	43.6	159.8	–
13	7.4132	6.8639	1758.8	1196.7	1445.2	1270.8	781.7	5.4	13.1	79.2	71.9	–	5.4	18.6	97.7	169.6	–

Table 2 Computed values of aquifer parameters

VES	Longitude (°E)	Latitude (°N)	$\rho_a(\Omega m)$	h_a (m)	Longitudinal conductance (Ω^{-1})	Transverse resistance (Ωm^2)	Hydraulic conductivity (m/day)	Transmissivity (m^2/day)	Protective capacity rating
1	7.4065	6.8585	4554.0	83.1	0.018	378,437.40	0.149	12.399	Poor
2	7.4127	6.8693	5713.9	104.6	0.018	597,673.90	0.121	12.629	Poor
3	7.4231	6.8613	4089.3	108.4	0.027	443,280.10	0.165	17.882	Poor
4	7.4267	6.8613	3211.7	109.8	0.034	352,644.70	0.207	22.692	Poor
5	7.4079	6.8691	2799.0	114.9	0.041	321,605.10	0.235	26.998	Poor
6	7.4222	6.8525	2339.0	137.3	0.059	321,144.70	0.278	38.144	Weak
7	7.4098	6.8596	1146.1	98.2	0.086	112,547.00	0.541	53.078	Weak
8	7.4089	6.8698	4261.6	117.2	0.028	499,459.50	0.159	18.604	Poor
9	7.4056	6.8681	1523.9	86.9	0.057	132,426.90	0.414	36.007	Weak
10	7.4123	6.8716	4191.5	184.3	0.044	772,493.50	0.161	29.711	Poor
11	7.4038	6.8719	2042.3	138.7	0.068	283,267.00	0.315	43.732	Weak
12	7.4105	6.8651	1246.8	116.1	0.093	144,753.50	0.500	58.011	Weak
13	7.4016	6.8589	1270.8	71.9	0.057	91,370.52	0.491	35.293	Weak

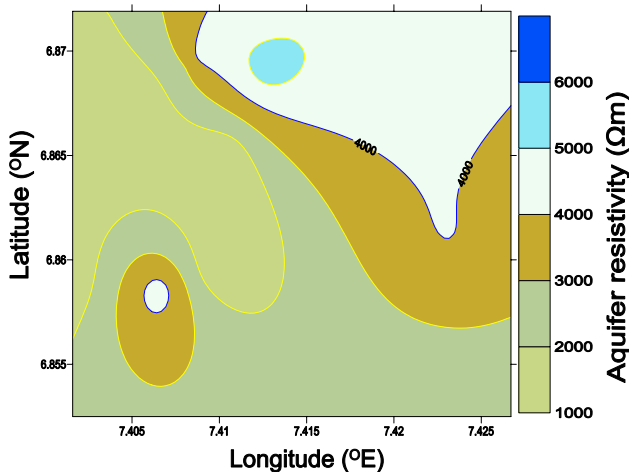


Fig. 5 Contour map of the study area showing the variation of aquifer resistivity

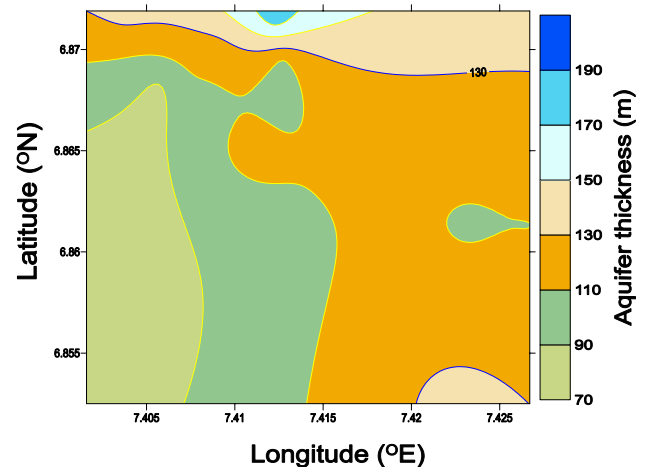


Fig. 6 Contour map of the study area showing the variation of aquifer thickness

can affect the groundwater repositories. The variation of hydraulic conductivity is displayed in Fig. 8. Low values of K span through the north and south of the study area while the high K values is observed in the western part of the study area. Areas with low hydraulic conductivity indicate the presence of less permeable earth materials compared to other areas.

The transmissivity of the aquifer layer has the same trend as hydraulic conductivity, as shown in the contour map (Fig. 9). This is an indication of the effect of hydraulic conductivity and thickness on transmissivity. Areas with low protective capacity and high transmissivity of the aquifer layer will support percolation and migration of contaminated fluids within the groundwater repositories.

Physical and geochemical results

Table 3 provides the results of water samples collected from five boreholes and analysed in order to obtain the concentrations of the physical and chemical parameters. The Total dissolved solute (TDS) with a range 70.30 to 79.08 mg/L and an average value of 75.22 mg/L, has values that fall below the WHO standard (WHO 2004). The TDS values are within the excellent class according to Rahman et al. (2015). The anions considered were SO_4^{2-} , Cl^- , NO_3^- and HCO_3^- and their concentrations determined. The SO_4^{2-} with a ranged of 3.26–5.86 mg/L and a mean value of 4.97 mg/L, Cl^- has values ranging from

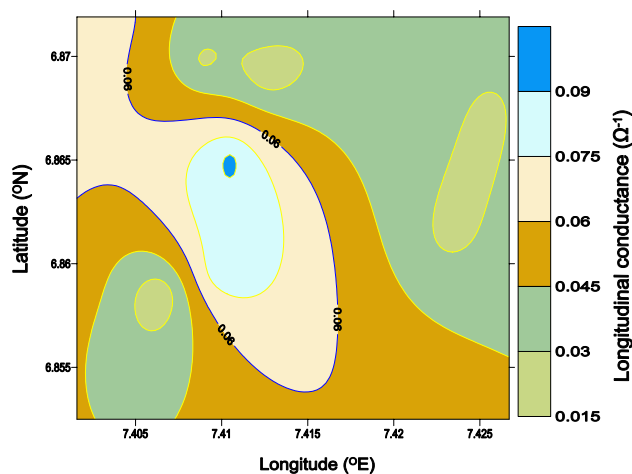


Fig. 7 Contour map of the study area showing the variation of longitudinal conductance

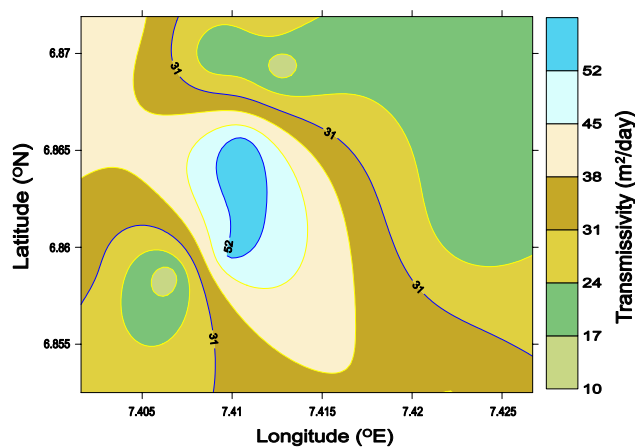


Fig. 9 Contour map of the study area showing the variation of transmissivity

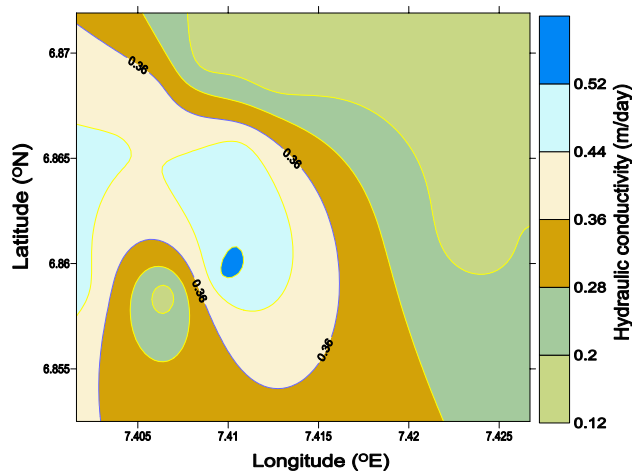


Fig. 8 Contour map of the study area showing the variation of hydraulic conductivity

21.30 to 34.08 mg/L and a mean value of 27.76 mg/L, NO_3^- with a range 5.59–9.09 mg/L has a mean value of 7.55 mg/L and HCO_3^- with a range of 0.80–2.40 mg/L and a mean value of 1.70 mg/L. The values of the anions were below the WHO standard limit. The order of abundance of anions is $\text{Cl}^- > \text{NO}_3^- > \text{SO}_4^{2-} > \text{HCO}_3^-$. The low concentration of anions in the water samples may be attributed to the low concentration of the minerals or rocks bearing these ions. The cations (K^+ , Na^+ , Ca^{2+} , Mg^{2+} and Fe^{2+}) were evaluated. K^+ with range of 1.86–5.88 mg/L and a mean value of 3.54 mg/L, Na^+ with a range of 0.64–1.50 mg/L and mean value of 1.02 mg/L, Ca^{2+} with range of 0.00–4.00 mg/L and mean value of 1.60 mg/L, Mg^{2+} with a range of 0.31–0.42 mg/L and mean value of

0.36 mg/L while Fe^{2+} with a range of 0.12–1.47 mg/L has a mean value of 0.98 mg/L. The order of abundance of cations is $\text{K}^+ > \text{Ca}^{2+} > \text{Na}^+ > \text{Fe}^{2+} > \text{Mg}^{2+}$. The concentration of the cations also falls below the WHO standard limit except Fe^{2+} that exceeds WHO standard in boreholes BH B, BH C and BH E. The high concentration of Fe^{2+} may be attributed to weathering of iron bearing minerals and rocks.

The suitability of groundwater for irrigation purposes was also evaluated using the concentrations of the ions of sodium, calcium, magnesium and potassium to determine the Magnesium Hazard (MH), Sodium Adsorption Ratio (SAR) and Sodium percentage (Na%) as presented in Table 4.

The result shows MH ranging of 7.81–100.00 with a mean value of 38.16, SAR ranging of 0.33–9.37 with a mean value of 2.69 and Na% ranging from 8.84 to 40.33 with a mean value of 18.31. According to Khodapanah et al. (2009) $\text{MH} > 50$ is not recommended for irrigation, hence groundwater in BH B is not suitable for irrigation since high value of Mg^{2+} in water increases soil pH and leads to decrease in the availability of phosphorus. The calculated values of SARS are all less than 10, as such the water samples falls within the ideal or excellent class which is good for irrigation according to the classification of Todd (1980) and Raju et al. (2011). The values of Na% according to Khodapanah et al. (2009) indicate that all the water samples except that of BH B have values $< 20\%$, which indicates excellent class. BH B with value within 20–40% falls within the good class. This is an indication of good soil properties and the boreholes have good irrigation groundwater which will encourage agricultural productivity.

Table 3 Results of chemical ions of water sample analysis

S/N	Parameter	BH A	BH B	BH C	BH D	BH E	Average	WHO (2004)
1	TDS (mg/L)	70.34	79.08	77.54	78.86	70.30	75.22	500.0
2	SO ₄ ²⁻ (mg/L)	3.26	5.76	5.76	4.22	5.86	4.97	400.0
3	Cl ⁻ (mg/L)	22.34	34.08	28.40	32.66	21.30	27.76	600.0
4	K ⁺ (mg/L)	2.94	1.86	4.80	5.88	2.24	3.54	30.0
5	Na ²⁺ (mg/L)	0.71	1.47	0.78	1.50	0.64	1.02	200.0
6	Ca ²⁺ (mg/L)	4.00	0.00	0.67	2.67	0.67	1.60	200.0
7	Mg ²⁺ (mg/L)	0.34	0.31	0.31	0.40	0.42	0.36	150.0
8	Fe ²⁺ (mg/L)	0.12	1.47	1.22	0.61	1.47	0.98	1.0
9	NO ₃ ⁻ (mg/L)	9.09	6.99	7.69	8.39	5.59	7.55	45.0
10	HCO ₃ ⁻ (mg/L)	0.80	2.20	2.00	1.10	2.40	1.70	500.0

Table 4 Estimated indicators from ions concentrations

S/N	Parameter	BH A	BH B	BH C	BH D	BH E	Average
1	MH	7.81	100.00	31.49	13.00	38.49	38.16
2	SAR	0.33	9.37	1.61	0.98	1.18	2.69
3	Na%	8.84	40.33	11.94	14.34	16.11	18.31

Conclusion

This study evaluates groundwater quality by means of an electrical resistivity technique and a geochemical method and also aims to assess its suitability for irrigation purposes. The VES involves thirteen sounding points and five subsurface layers were obtained from which hydrogeological characteristics were delineated. The result revealed the variation of resistivity within the subsurface, with deeper layers having higher resistivity values compared to the upper layers, which may be influenced by contaminants infiltrating through the vadose zone. The longitudinal conductance reveals the protective capacity as poor-weak and renders the aquifer repositories liable to contamination, while the hydraulic conductivity determines the extent of permeability of the subsurface, as areas with high hydraulic conductivity will ease the movement of geofluids through the subsurface. The laboratory analysis was carried to determine the concentration of TDS, some anions (SO₄²⁻, Cl⁻, NO₃⁻ and HCO₃⁻) and cations (K⁺, Na²⁺, Ca²⁺, Mg²⁺ and Fe²⁺) in groundwater samples of five boreholes. The results reveal that the parameters have concentration below the limit as per WHO standard except Fe²⁺ that exceeds WHO standard in some boreholes. The MH, SAR and Na% results showed that the groundwater in the study area is good and in excellent class for irrigation. It is recommended that future research work be carried out to evaluate the seasonal variations of the hydrogeochemical facies and consider other indices such as the water quality index, contamination factor, and pollution load index of

groundwater in the study area. Also, we recommend that salinity hazard, sodium hazard, alkalinity, Specific ions should be considered to confirm the suitability of water for irrigation.

Acknowledgements The authors are thankful to Tetfund (TETFUND/DR&D/CE/UNI/NSUKKA/RP/VOL.I) for sponsoring this research.

Declarations

Conflict of interest The authors declare that they have no conflicts of interest.

References

- Akpan, A. E., Ugbaja, A. N., & George, N. J. (2013). Integrated geophysical, geochemical and hydrogeological investigation of shallow groundwater resources in parts of the Ikom-Mamfe Embayment and the adjoining areas in Cross River State Nigeria. *Environment and Earth Science*, 70(3), 1435–1456.
- Aleke, C. G., Ibuot, J. C., & Obiora, D. N. (2018). Application of electrical resistivity method in estimating geohydraulic properties of a sandy hydrolithofacies: A case study of Ajali Sandstone in Ninth Mile, Enugu State, Nigeria. *Arabian Journal of Geosciences*, 11, 322.
- Chandra, S., Singh, P. K., Tiwari, A. K., Panigrahy, B., & Kumar, A. (2015). Evaluation of hydrogeological factor and their relationship with seasonal water table fluctuation in Dhanbad district, Jharkhand, India. *ISH Journal of Hydraulic Engineering*, 21, 193–206.
- Choudhury, K., & Saha, D. K. (2004). Integrated geophysical and chemical study of saline water intrusion. *Groundwater*, 42, 671–677.

- Ekanem, A. M., Akpan, A. E., George, N. J., & Thomas, J. E. (2021). Appraisal of protectivity and corrosivity of surficial hydrogeological units via geo-sounding measurements. *Environmental Monitoring and Assessment*, 193, 718. <https://doi.org/10.1007/s10661-021-09>
- Ganiyu, S. A., Badmus, B. S., Oladunjoye, M. A., Aizebeokhai, A. P., & Olurin, O. T. (2015). Delineation of leachate plume migration using electrical resistivity imaging on Lapite dumpsite in Ibadan. *Southwestern Nigeria, Geosciences*, 5(2), 70–80.
- George, N. J. (2021). Integrating hydrogeological and second-order geo-electric indices in groundwater vulnerability mapping: A case study of alluvial environments. *Applied Water Sciences*, 11, 123. <https://doi.org/10.1007/s13201-021-01437-x>
- George, N. J., Akpan, A. E., & Evans, U. F. (2016). Prediction of geo-hydraulic pore pressure gradient differentials for hydrodynamic assessment of hydrogeological units using geophysical and laboratory techniques: A case study of the coastal sector of Akwa Ibom State, Southern Nigeria. *Arabian Journal of Geosciences*, 9(4), 1–13.
- George, N. J., Ibang, J. I., & Ubom, A. I. (2015). Geoelectrohydrogeological indices of evidence of ingress of saline water into freshwater in parts of coastal aquifers of Ikot Abasi, southern Nigeria. *Journal of African Earth Sciences*, 109, 37–46.
- Hossain, M. L., Das, S. R., & Hossain, M. K. (2014). Impact of landfill leachate on surface and groundwater quality. *Journal of Environmental Science and Technology*, 7, 337–346.
- Ibuot, J. C., & Obiora, D. N. (2021). Estimating geohydrodynamic parameters and their implications on aquifer repositories: A case study of University of Nigeria, Nsukka, Enugu State. *Water Practice and Technology*, 16(1), 162–181.
- Ibuot, J. C., Okeke, F. N., George, N. J., & Obiora, D. N. (2017). Geophysical and physicochemical characterization of organic waste contamination of hydrolithofacies in the coastal dumpsite of Akwa Ibom State, Southern Nigeria. *Water Science and Technology: Water Supply*, 17(6), 1626–1637.
- Ibuot, J. C., Okeke, F. N., Obiora, D. N., & George, N. J. (2019). Assessment of impact leachate on hydrogeological repositories in Uyo, Southern Nigeria. *Journal of Environmental Engineering and Science*, 14(2), 97–107.
- Khodapanah, L., Sulaiman, W. N. A., & Khodapanah, N. (2009). Groundwater quality assessment for different purposes in Eshtehard district, Tehran, Iran. *European Journal of Scientific Research*, 36(4), 543–553.
- Obaje, N. G. (2009). *Geology and mineral resources of Nigeria*. Springer.
- Obiora, D. N., Ajala, A. E., & Ibuot, J. C. (2015). Evaluation of aquifer protective capacity of overburden units and soil corrosivity in Makurdi, Benue State, Nigeria, using electrical resistivity method. *Journal of Earth System Science*, 124(1), 125–135.
- Obiora, D. N., & Ibuot, J. C. (2020). Geophysical assessment of aquifer vulnerability and management: A case study of University of Nigeria, Nsukka, Enugu State. *Applied Water Science*, 10, 29. <https://doi.org/10.1007/s13201-019-1113-7>
- Obiora, D. N., Ibuot, J. C., & George, N. J. (2016). Evaluation of aquifer potential, geoelectric and hydraulic parameters in Ezza north, Southeastern Nigeria, using geoelectric sounding. *International Journal of Environmental Science and Technology*, 13(2), 435–444.
- Oguama, B. E., Ibuot, J. C., Obiora, D. N., & Udofia, M. U. (2019). Geophysical investigation of groundwater potential, aquifer parameters, and vulnerability: A case study of Enugu State College of Education (Technical). *Modeling Earth Systems and Environment*, 5(3), 1123–1133.
- Oladapo, M. I., Mohammed, M. Z., Adeoye, O. O., & Adetola, O. O. (2004). Geoelectric investigation of the Ondo State Housing Corporation Estate; Ijapo, Akure, Southwestern Nigeria. *Journal of Mining and Geology*, 40, 41–48.
- Omeje, E. T., Ugbor, D. O., Ibuot, J. C., & Obiora, D. N. (2021). Assessment groundwater repositories in Edem, Southern Nigeria, using vertical electrical sounding. *Arabian Journal of Geosciences*, 14, 421.
- Raghunath, H. M. (1987). *Groundwater* (2nd ed., pp. 344–369). New Delhi: Wiley.
- Rahman, M. A., Md. Islam, M. M., & Ahmed, F. (2015). Physico-chemical and bacteriological analysis of drinking tube-well water from some primary school, Magura, Bangladesh to evaluate suitability for students. *International Journal of Applied Sciences and Engineering Research*, 4(5), 735–749.
- Raju, N. J., Shukla, U. K., & Ram, P. (2011). Hydrogeochemistry for the assessment of groundwater quality in Varanasi: A fast-urbanizing center in Uttar Pradesh, India. *Environmental Monitoring and Assessment*, 173, 279–300.
- Reyment, R. A. (1965). *Aspects of the geology of Nigeria*. Ibadan University Press.
- Simpson, A. (1954). The Nigeria coalfield. The geology of parts of onitsha, owerri and benue provinces. *Bulletin Geological Survey Nigeria*, 24, 1–85.
- Sisir, K. N., & Anindita, L. (2012). Hydrochemical characteristics of groundwater for domestic and irrigation purposes in Dwarakeswar Watershed Area, India. *American Journal of Climate Change*, 1, 217–230.
- Thomas, J. E., George, N. J., Ekanem, A. M., & Nsikak, E. E. (2020). Electrostratigraphy and hydrogeochemistry of hyporheic zone and water-bearing caches in the littoral shorefront of Akwa Ibom State University, Southern Nigeria. *Environmental Monitoring and Assessment*, 192, 505. <https://doi.org/10.1007/s10661-020-08436-6>
- Verma, P., Singh, P. K., Sinha, R. R., & Tiwari, A. K. (2020). Assessment of groundwater quality status by using water quality index (WQI) and geographic information system (GIS) approaches: A case study of the Bokaro district, India. *Applied Water Science*, 10(27), 7. <https://doi.org/10.1007/s13201-019-1088-4>
- World Health Organization. (2004). *Guidelines for drinking-water quality*. World Health Organization.
- Yan, C. A., Zhang, W., Zhang, Z., Liu, Y., Deng, C., & Nie, N. (2015). Assessment of water quality and identification of polluted risky regions based on field observations and GIS in the Honghe River Watershed, China. *PLoS One*, 10(3), 0119130.